CEIG - Spanish Computer Graphics Conference (2014)
Pere-Pau Vázquez and Adolfo Muñoz (Editors)

Image-Based Flow Transfer

Carles Bosch* and Gustavo Patow

ViRVIG-UdG, Universitat de Girona, Girona, Spain

Figure 1: *Flow transfer. From left to right, input flow stain, target image, and two examples of user-directed flow transfer. Observe how the flow properly adapts to the target surface.*

Abstract

Weathering phenomena are ubiquitous to urban environments. In particular, fluid flow becomes a specially representative but difficult phenomenon to reproduce. In order to produce realistic flow effects, it is possible to take advantage of the widespread availability of flow images on the internet, which can be used to gather key information about the flow. In this paper we present a technique that allows transferring flow phenomena between photographs, adapting the flow to the target image and giving the user flexibility and control through specifically tailored parameters. This is done through two types of control curves: a fitted theoretical curve for the mass of deposited material, and a control curve extracted from the images for the color. This way, the user has a set of simple and intuitive parameters and tools to control the flow phenomena on the target image. To illustrate our technique, we present a complete set of images that somewhat cover a large range of flow phenomena in urban environments.

Categories and Subject Descriptors (according to ACM CCS): I.3.3 [Computer Graphics]: Picture/Image Generation—Line and curve generation, Bitmap and framebuffer operations

1. Introduction

Weathered surfaces are ubiquitous in urban environments, and modeling them is a key issue for achieving realistic urban landscapes. Among the effects to consider, weathering produced by fluid flow is one of the most important ones because of its universality and large scale effects. Also, it is particularly difficult to model because it is strongly shape-dependent: global shape affects the overall direction of flow, while small scale roughness (details or micro-geometry) and porosity alters its look and behavior [DPH96].

With the widespread use of digital photography, it is now not difficult to find thousands of images showing weathering effects. Up to now, the only use that has been given to this resource is the extraction of some guiding parameters for

DOI: 10.2312/ceig.20141110

a particle-based simulation [BLR*11]. However, little has been done to use the images to transfer the weathering effects *themselves*.

In this paper we propose a new method for transferring weathering phenomena between images that focus on easily controlling the underlying transport effects. Our method recovers a set of intuitive but physically-based parameters that allow easy modification of the transferred phenomenon, coupled with appropriate tools for adapting the underlying effect onto new targets. This way, the user can simply perform a *copy & paste*-like operation of the flow effects from the samples onto new images, being able to intuitively control the final result, as can be seen in Figure 1. We can summarize our contributions as:

- A new image-based method to transfer flow weathering phenomena that allows the adaptation of the original color and detail.
- An intuitive control system based on fitting an analytical model that lets users modify and adapt the flow to different conditions.

2. Previous work

Dorsey et al. presented one of the first works to deal with stains by fluid flow [DPH96], using a simulation with particle systems to recreate the flow effects. Chen et al. [CXW*05] proposed γ-ton tracing, based on tracing a special kind of aging-inducing particles and accumulating their contributions. Mérillou et al. [MMG*10] incorporated flow accessibility as a measure to limit stain distribution. Recently, Bosch et al. [BLR*11] extracted parameters of a particle-based simulation from real photographs along with detail maps. None of these works directly transferred flow stains from pictures, using them only to extract simulation parameters at most. For an extense review of weathering simulation in Computer Graphics, we refer the interested reader to the survey by Mérillou et al. [MG08] or the excellent book by Dorsey et al. [DRS08].

Image-based techniques are closely related with the one we present here. Oh et al. [OCDD01] allowed relighting, content removal and editing in 3D, as well as viewpoint changes, based on reconstructing and editing depth and color maps from single uncalibrated images. Sloan et al. [SMGG01] developed a technique for capturing custom artistic shading samples from art work to allow users to generate shading models with similar light, depth, and material properties as accomplished by artists. Fang and Hart [FH04] proposed to split the image in patches and synthesized the texture for each one, while Khan et al. [KRFB06] used image-processing techniques to edit the image. Winnemoller et al. [WOBT09] applied parallax mapping to an image and its depth map obtained from its normals. Recently, Yeung et al. [YTBK11] presented a method that allows the users to sketch distortion patterns resulting from refraction effects.

Wang et al. [WTL*06] synthesized weathering patterns from given examples by creating a basis of weathering samples (an appearance manifold) that approximated the space of weathered surfaces. Xue et al. [XWT*08] continued this research to achieve interactive edition and performed simple transfer of effects between images, but without extending their work to deal with geometric variations or flow-produced stains. Later on, Xue et al. [XDR11] developed a method for simulating stone erosion in a photograph. Although practical, none of these approaches deal with the kind of natural phenomena we aim at transferring with our approach.

Our work also relates to flow synthesis algorithms like the work of Neyret [Ney03]. Neyret proposed to advect textures by combining layers of advected parameterizations according to a criterion based on the local accumulated deformation. These layers were periodically regenerated. Kwatra et al. [KEBK05] defined texture synthesis as a minimization problem, adding control through constraints like flow and color. For flows, they used the previous frame as a constraint for synthesizing the current one, achieving flow continuity. Later, Kwatra et al. [KAK*07] synthesized textures over dynamical fluid surfaces by transporting texture information.

Related to the goal of this paper, Treuille et al. [TMPS03] presented a method to control the keyframes of smoke simulations. Later on, Bhat et al. [BSHK04] presented an algorithm for synthesizing and editing video of natural phenomena exhibiting continuous flow patterns. The method analyzed the trajectory of particles with the aid of user-provided guiding lines. Okabe et al. [OAIS09] presented a method to design a continuous flow animation by using video examples. Following this work, Okabe et al. [OAO11] used a video database to generate fluid animation from a single image. These works mainly rely on video sequences and do not consider material *deposition* because of flow mechanisms, as we do here.

In terms of acquisition, Hasinoff et al. [HK07] reconstructed visually realistic 3D models of dynamic semitransparent scenes (e.g., fire) from a very small set of simultaneous views. Wang et al. [WLZ*09] proposed a system to acquire water animations by combining video-extraction and water-surface optimization.

3. Overview

Our aim is to transfer the result of a flow-based staining process from an input image to a target one. The key realization in our system is that this transfer can be done by extracting and "cleaning" the input stains from any dependence on the input background, and later blend it with the background at the target image. Our pipeline for transferring flow effects is divided in two stages: extraction and transfer. For the sake of clarity, we subdivide the explanations of the former stage in three steps (i.e., computation of the concentration map,

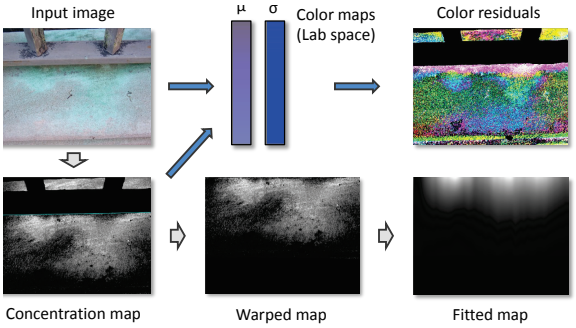

Figure 2: *Feature extraction. Top: Given an input image and its concentration map Δ, we extract its color map C^{μ}, its variance map C^{σ} and the residual r (in false color). Bottom: the concentration map is warped to obtain a straight source edge, from which we fit the theoretical curves.*

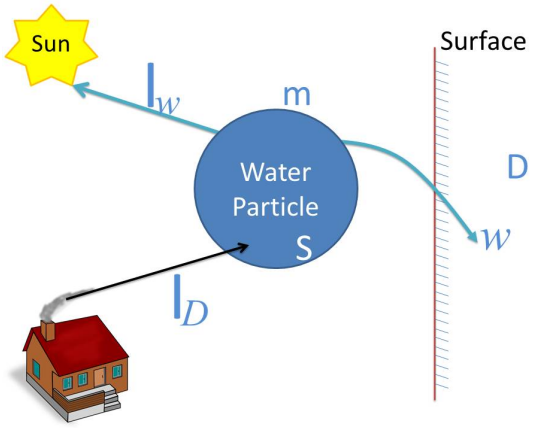

Figure 3: *Fundamental elements for absorption and sedimentation. Adapted from [DPH96].*

parameter estimation and color extraction); and the latter in three further steps: basic transfer, geometric details and stain editing.

The user input required by this process is limited, as it only consists of a set of regions selecting the background vs. flow colors in the input image (Section 4.1), the starting of the flow in both images by means of two polylines (Section 4.2 and 5.1), and the tuning of parameters for editing the final flow (Section 5.3).

4. Flow extraction

Flow extraction is a process that aims at identifying the stained area and extracting its controlling parameters. For this, we compute two types of curves from the input flow image: one controlling the concentration of material deposited by the process, obtained through fitting a set of theoretical curves to a *concentration map*; and another controlling its color, obtained directly from the stained area in the input image and represented as a sampled *color map* C^{μ}. See Figure 2.

4.1. Concentration map

The *concentration map* $\Delta(x)$ defines the amount of material deposited at each point in the image, which we assume to be related to its color opacity or mixture between the stain and background colors. To generate such a map, we can resort to techniques such as appearance manifolds [WTL*06] or alpha-matting techniques [WC07]. In our case, we use the former method, which is specially tailored to weathering phenomena. Given two regions of pixels selected in the image, representing the most and least weathered points, we use the appearance manifold to obtain the corresponding weathering map, which is here used as our concentration map $\Delta(x)$. As in [WTL*06], we assume that $\Delta(x) \in [0,1]$, with 0 representing the least stained points and 1 the most stained ones.

4.2. Parameter estimation

In order to control the flow pattern during the transfer, we fit a set of control curves to the concentration map, which will approximate the distribution of concentration over the surface. These curves are physically-based and derived from models of water absorption and material deposition, as described next.

The fundamental equations for absorption and sedimentation are well known [DPH96]. The absorption of water at a surface depends on the material properties, like porosity and available void space. For absorption, the governing equations are presented in Equation 1.

$$\begin{aligned} \frac{\partial m}{\partial t} &= -k_a \frac{a-w}{a} m \\ \frac{\partial w}{\partial t} &= k_a \frac{a-w}{a} - I_w \end{aligned} \tag{1}$$

There, m is the water content in the water particles (droplets), w is the water absorbed at the material surface, a is the absorption, k_a is the absorptivity, and I_w is the evaporation, which we assume to be negligible for the processes described here. The amount of water absorbed w depends mainly on the absorptivity k_a and the duration of the exposure (represented by ∂t), which in turn is limited by the absorption a. See Figure 3.

There is a number of possible approximations for the set of Equations 1 [FX94]. We have decided to use one of the most accurate ones [Wit05, SRLW13], which is a simple solution in terms of the $erfc$ function, defined as

$$erfc(x) = 1 - erf(x) = \frac{2}{\sqrt{\pi}} \int_x^{\infty} e^{-t^2} dt$$

so we decided to use a function of the shape

$$w(x) = \alpha \cdot erfc(\gamma x)$$

for the fluid flow, with α and γ two constants that depend on the material surface.

On the other hand, sedimentation is the process of substance deposition on the surface, like dirt or pollution. The governing equations are presented in Equation 2, where S is the concentration of dissolved material, D is the concentration of material deposited at the surface, k_s is adhesion rate, k_D is solubility rate, and I_D the deposit coefficient from the modeled phenomenon, again considered to be null during flow for the purposes of this work [DPH96].

$$\begin{aligned} \frac{\partial S}{\partial t} &= -k_s \cdot S + k_D \cdot D \cdot \frac{A}{m} \\ \frac{\partial D}{\partial t} &= k_s \cdot S \cdot \frac{m}{A} - k_D \cdot D + I_D \end{aligned} \tag{2}$$

This second set of equations for sedimentation can be solved analytically by assuming a constant factor between the contact area A and the particle water content m (i.e., $A/m = constant$). From the second equation in Equation 2, we get that

$$S = \frac{1}{k_s'}\left(\frac{\partial D}{\partial t} + k_D D\right)$$

with $k_s' = k_s * m/A$. Inserting this into the first equation leads to:

$$\frac{\partial^2 D}{\partial t^2} + (k_D + k_S^2 * m/A)D = 0$$

This is a simple second order differential equation, which can be solved, leading to an exponential expression. By assuming a linear relationship between time and the distance traveled by the droplet, we arrive at an expression of the form:

$$D(x) = \phi e^{-\beta x}$$

where ϕ and β are two constants related to the materials. ϕ and β parameters can be easily estimated using standard linear regression in log space, which we apply to each stain column in order to capture the concentration variability $D(x)$ along the source. This step is done after warping the concentration map according to the user-defined polyline representing the stain source in the image (see Figures 2 and 4).

In Figure 5 we can see an example of the process of fitting a curve to an input stain (oxide on a rough wall surface). From left to right, the input image, the corresponding concentration map, the fitted pattern with one column highlighted in green, and the pattern applied to an image. At the bottom row, we can see the fitted curve (orange line) obtained from the corresponding concentration profile (purple profile). The fitting may not be very accurate in some situations, especially under the presence of strong surface variations. However, these profiles are only used to modify the concentration map, and thus the final result still preserves the original detail (top row, two rightmost images). In Section 5.3 we explain how a global controlling mechanism is used to alter this map.

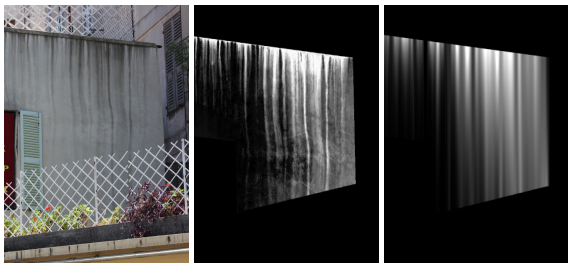

Figure 4: *Parameter fitting. Given an input image (left), we extract its concentration map (middle) and fit an analytical curve for each pixel along the source (right). The parameters of these curves will be globally controlled during the editing phase.*

4.3. Color extraction

As we are going to transfer the stains to new photographs, and thus to new materials, we need to extract not only the stain shapes, but also their colors, and transfer them as well. For that, we compute a control curve, called *color map* (C^{μ}), that relates concentration values with stain colors, similar to [BLR*11]. This color map is a function of the concentration Δ and represents the average color associated to each concentration value. The resulting functions $L(\Delta)$, $a(\Delta)$ and $b(\Delta)$ (in *Lab* color space) evaluate these curves for a given concentration value Δ. Along with the color map, we compute a variance map C^{σ} as well. The color map can be understood as a sampled curve that can be globally scaled or modified, allowing some global color control. The variance map will account for the variability of colors associated to each average color, and will be used to better preserve the original texture during the transfer, as described in the next section.

These maps, although very useful for a simple direct mapping, might not provide enough precision for a complex stain pattern. In order to account for this complexity, we also compute a *residual map* r as

$$r(x,y) = InputImage(x,y) - C^{\mu}(\Delta(x,y))$$

where $r(x,y)$ is the residual *Lab* color of the pixel at position (x,y). See Figure 2.

5. Flow transfer

5.1. Basic transfer

Using the information extracted from the input image, we can proceed to transfer the flow weathering effect to a new

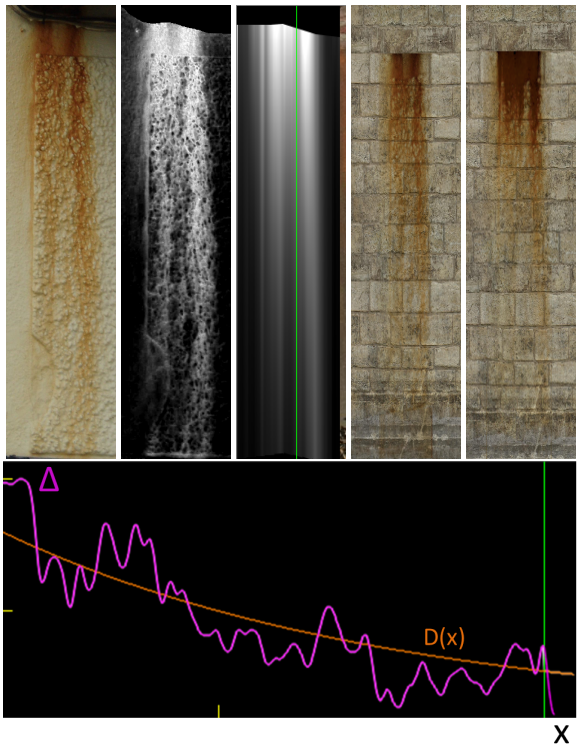

Figure 5: *Fitting and transfer of flow. Top, from left to right: input image, extracted concentration map, fitted model, and two edits performed after transferring the original map onto the target image. Bottom: concentration and fitted profile for the column shown in the top-middle image (Δ and $D(x)$, with x measured along the flow). Even if the fitting is not perfect, the resulting images (top rightmost images) are still of high quality: the stain has been stretched in the first case (smaller β) and its concentration has been increased in the latter (larger ϕ).*

target image. The inputs needed from the target in the most basic setup are the color information, provided by the target image, and a hand drawn polyline indicating where the flow will originate on this image. The user-provided polyline is used to warp the concentration map from the input image to the target one, so that the edges on the source match the ones defined on the target. As a consequence, this generates a new concentration map Δ'. We perform this warping by means of a perspective transformation [Ope13].

Given Δ', we also need to transfer the color information from the input image. This transfer should take care of preserving all the colors associated to the input weathering effect while removing any trace from the original background. Bosch et al. [BLR*11] proposed a simple approach to transfer this color information by properly pixel-wise scaling the colormap from the original background color to the new one. We found this approach to work well for stains with similar chroma variations associated to each degree. However, stains containing non-uniform mixtures of colors can not be well represented with a single one dimensional curve [ATDP11]. In addition, the input concentration map often suffers from bad color clusterings for similar degrees.

To solve this, we add onto the obtained color the residual color extracted from the preprocessing step, properly weighted by the variance (standard deviation) associated to each weathering concentration. The rationale behind this is that the residual cannot be directly added to any concentration value, as the residual might have an original scale that could be too large for the target weathering. As a consequence, we decided to attenuate the residuals with the variance map C^σ to guarantee a proper contribution. As we also want to maintain color variations at the highest concentration levels, but not for the background, we also scale this deviation by the concentration itself, so that the deviation tends to zero towards the background color. The target weathering color $I'(x,y)$ is computed from its original color, $I(x,y)$, as:

$$I'(x,y) = s(x,y)C^\mu(\Delta'(x,y)) + r'(x,y)C^\sigma(\Delta'(x,y))\Delta'(x,y),$$

where $s(x,y)$ is the scaling applied to the color map to warp it according to the color of the target pixel, C^σ is the variance of the color map, and $r'(x,y)$ is the residual of the current pixel, transferred along with the concentration map. s is computed as [BLR*11]:

$$s(x,y) = \frac{I(x,y) - C^\mu(1)}{C^\mu(0) - C^\mu(1)}$$

This transformation is done in *Lab* color space and independently for each channel, which produces better results than RGB [XWT*08]. Observe that the target image color is introduced in the above expressions through the function $s(x,y)$, which includes its color ($I(x,y)$).

5.2. Geometric details

Adapting the color is essential for properly transferring a weathering effect. However, the concentration map also needs to be adapted, as it is typically perturbed by the geometric details of the underlying surface. Here we consider that these details alter the concentration along the propagation direction without modifying this direction significantly. This effect is mostly due to small-scale details, which usually come in the form of high frequency variations. In order to reproduce them, we can thus simply modify the concentration according to the high frequency geometric changes present on the target surface.

To capture the geometric changes of the target surface, the user could provide a depth map or compute it by means of shape-from-shading techniques [ZTCS99]. In our case, we use a similar strategy than Khan et al. [KRFB06] and Oh et al. [OCDD01], and assume that depth is inversely related to image luminance. This way, we can automatically generate

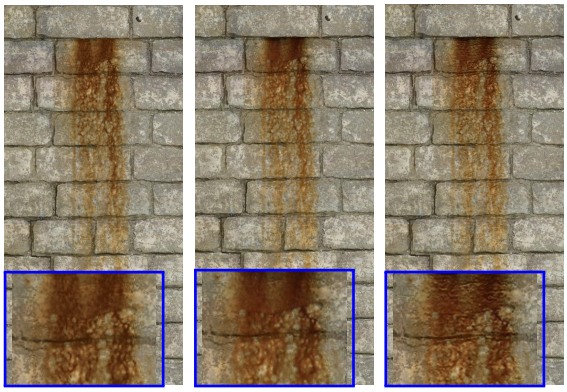

Figure 6: *From left to right: simple color warping [BLR*11], our approach, and our approach adding surface details.*

a depth map from the image intensity. This method has the well-known limitation that the light direction in the input image affects the geometry extraction, and it is not possible to know whether a part of the image has a positive or a negative slope. A better but slower method would be to use a light estimation method followed by a more sophisticated shape-from-shading approach [LMGH*13, WH97].

After computing the depth map, we extract the high-frequencies as the difference between this map and a low-pass Gaussian filtered version. We let the user specify the size of the details to be incorporated, and hence the size of the filtering kernel. The differential of the resulting map along the propagation direction (vertical direction on warped space) is used to compute the new concentration, using the following expression:

$$\Delta'(x,y) = \Delta'(x,y) + \mathcal{G}(\Delta'(x,y), \frac{1}{2}, \frac{1}{6})\, \delta_y Z_h(x,y)$$

where $Z_h(x,y)$ is the high-pass filtered depth map and $\mathcal{G}(x,\mu,\sigma)$ is a Gaussian function that attenuates the perturbations on the limits of the concentration map ($[0,1]$). For us, the value of $\sigma = 1/6$ worked remarkably well, but other expressions could also provide good results. Since the input concentration map already contains perturbations due to the details on the original surface, we similarly apply a Gaussian filter in the input map in order to remove the corresponding high-frequency details.

At Figure 6, we can see an example comparing the results obtained by Bosch et al. [BLR*11] with our own, with and without taking into account the surface details.

5.3. Stain editing

To give the user the freedom to change the concentration of the transferred stain, we allow changing the sedimentation coefficients of the profiles fitted to Δ. To do this we express

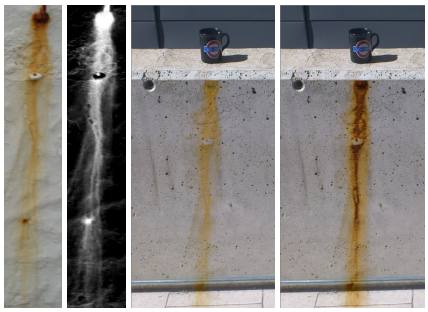

Figure 7: *Rust examples. From left to right, input image, concentration map, and two applications of the stain to a clean wall.*

each column of pixels in the input image as a profile defined by the basis function D plus some residual values r that are characteristic of the stain pattern, as described in Section 4.3. By changing the estimated profile parameters ϕ and β, we can easily modify the corresponding concentration. In our implementation, the user is able to freely modify ϕ and β by means of two global scaling factors associated to each parameter, w_ϕ and w_β, as $\phi' = w_\phi \cdot \phi$ and $\beta' = w_\beta \cdot \beta$. These modifications are applied on the concentration map defined in input warped space, and sent through the transfer pipeline as detailed before. Each concentration profile $\Delta_x(y)$ is now modified using the following expression:

$$\Delta'_x(y) = D_x(y,\phi',\beta') + r_x(y) min(\frac{D_x(y,\phi',\beta')}{D_x(y,\phi,\beta)}, 1)$$

Here, ϕ is roughly related to the amount of material that is dragged and deposited with the flow, and β controls the reach of the flow. By fitting these two parameters in the original profiles and subsequently modifying them, we can thus easily alter the original concentration map. At Figure 5 we can see an example of the type of control these parameters add: at the top row, rightmost two images, the stain has been stretched (smaller β) and its concentration has been increased (larger ϕ), respectively.

6. Results

We have tested our technique over a set of images that cover a considerable range of flow phenomena in urban environments. In Figure 1 we transfer a complex biological growth pattern between two different types of stones. The biological stain was extracted from a photograph of a wall, and then applied to a clean stone building.

In Figure 7 we can see an input photograph with rust formed by a nail in a wall along with its concentration map, which are used to stain a clean concrete wall. Observe how the same pattern is modified by varying the amount of material (ϕ parameter), simulating its propagation over time.

Finally, in Figure 8 we can see a biological growth stain

Figure 8: *Chapel example: different applications of flow stains on a chapel image, including a biological stain and two moisture stains.*

and two moisture flows applied to a medieval chapel, placed at different positions and with different concentration parameters.

With respect to our actual implementation, the system is fully implemented in unoptimized C++ using the OpenCV library [Ope13] and it runs at interactive frame-rates. In our experience, each computation roughly takes less than one second, with a linear dependence on the number of pixels to be processed.

7. Discussion and Future Work

Tuning the parameters in our system is an easy and intuitive task, which is quite different to what happens with other methods like particle-based ones. Fitting the parameters of the concentration curve can be tricky in some situations, as there could be external factors like the superposition of additional phenomena or strong perturbations due to the original surface. However, even if the curve fitting does not exactly match the sampled values, its usage is reserved to the editing of the concentration map, not to replace the map itself. Modifying the concentration based on these control curves generally gives highly realistic results, as can be seen in the accompanying figures (e.g. Figure 5), thus showing the robustness of our system.

It is well known that running times for particle simulations can be long, mainly due to the particle-surface collision detection [BLR*11]. Our approach avoids all these computations by working directly in image space and not resorting to any kind of simulation at all. Besides this, our model to control the flow patterns is physically-based, as it is derived from state-of-the-art approximation models. We believe this simple model could also be useful to generate new stains from scratch, in order to easily simulate different stains produced by flow.

An interesting avenue for future work is to take into account the underlying geometry of the target image, as the stain shape is strongly related to it and thus might cause transfer artifacts. Another avenue is to provide the user with tools to edit not only the amount of material and the reach of the flow, but also the color properties of the deposited materials. Our current method does not rely on any texture synthesis approach, so the extensions to surfaces far from the original input on the image might produce noticeable artifacts if the original detail is to be fully preserved. Adding detail through synthesis is a promising way to solve this issue.

Finally, we would also like to extend this approach to simulate other transport phenomena. We believe our pipeline could be easily adapted by simply finding an adequate profile model that could be fitted to other examples, in order to cover a broader range of phenomena.

Acknowledgements

This work was partially funded by the TIN2010-20590-C02-02 project from the Ministerio de Ciencia e Innovación, Spain, and done with the support of the Comissionat per a Universitats i Recerca from the Departament d'Innovació, Universitats i Empresa of the Generalitat de Catalunya and the European Union.

*Carles Bosch is currently at Fundació Barcelona Media, Barcelona, Spain.

References

[ATDP11] AN X., TONG X., DENNING J. D., PELLACINI F.: Appwarp: retargeting measured materials by appearance-space warping. *ACM Trans. Graph. 30*, 6 (Dec. 2011), 147:1–147:10. 5

[BLR*11] BOSCH C., LAFFONT P.-Y., RUSHMEIER H., DORSEY J., DRETTAKIS G.: Image-guided weathering: A new approach applied to flow phenomena. *ACM Trans. Graph. 30*, 3 (May 2011), 20:1–20:13. 2, 4, 5, 6, 7

[BSHK04] BHAT K. S., SEITZ S. M., HODGINS J. K., KHOSLA P. K.: Flow-based video synthesis and editing. *ACM Trans. Graph. 23*, 3 (Aug. 2004), 360–363. 2

[CXW*05] CHEN Y., XIA L., WONG T.-T., TONG X., BAO H., GUO B., SHUM H.-Y.: Visual simulation of weathering by γ-ton tracing. *ACM Trans. Graph. 24*, 3 (July 2005), 1127–1133. 2

[DPH96] DORSEY J., PEDERSEN H. K., HANRAHAN P.: Flow and changes in appearance. In *Proceedings of the 23rd annual conference on Computer graphics and interactive techniques* (1996), SIGGRAPH '96, ACM, pp. 411–420. 1, 2, 3, 4

[DRS08] DORSEY J., RUSHMEIER H., SILLION F.: *Digital Modeling of Material Appearance*. Morgan Kaufmann Publishers Inc., San Francisco, CA, USA, 2008. 2

[FH04] FANG H., HART J. C.: Textureshop: texture synthesis as a photograph editing tool. *ACM Trans. Graph. 23*, 3 (Aug. 2004), 354–359. 2

[FX94] FREDLUND D., XING A.: Equations for the soil-water characteristic curve. *Canadian Geotechnical Journal 31*, 4 (1994), 521–532. 3

[HK07] HASINOFF S. W., KUTULAKOS K. N.: Photo-consistent reconstruction of semitransparent scenes by density-sheet decomposition. *IEEE Transactions on Pattern Analysis and Machine Intelligence 29*, 5 (2007), 870–885. 2

[KAK*07] KWATRA V., ADALSTEINSSON D., KIM T., KWATRA N., CARLSON M., LIN M. C.: Texturing fluids. *IEEE Trans. Vis. Comput. Graph. 13*, 5 (2007), 939–952. 2

[KEBK05] KWATRA V., ESSA I., BOBICK A., KWATRA N.: Texture optimization for example-based synthesis. *ACM Trans. Graph. 24*, 3 (July 2005), 795–802. 2

[KRFB06] KHAN E. A., REINHARD E., FLEMING R. W., BÜLTHOFF H. H.: Image-based material editing. *ACM Trans. Graph. 25*, 3 (July 2006), 654–663. 2, 5

[LMGH*13] LOPEZ-MORENO J., GARCES E., HADAP S., REINHARD E., GUTIERREZ D.: Multiple light source estimation in a single image. *Computer Graphics Forum 32*, 8 (2013), 170–182. 6

[MG08] MÉRILLOU S., GHAZANFARPOUR D.: A survey of aging and weathering phenomena in computer graphics. *Computers & Graphics 32*, 2 (2008), 159–174. 2

[MMG*10] MERILLOU N., MERILLOU S., GHAZANFARPOUR D., DISCHLER J.-M., GALIN E.: Simulating Atmospheric Pollution Weathering on Buildings. In *WSCG* (2010), pp. 65–72. 2

[Ney03] NEYRET F.: Advected textures. In *Proceedings of the 2003 ACM SIGGRAPH/Eurographics symposium on Computer animation* (Aire-la-Ville, Switzerland, Switzerland, 2003), SCA '03, Eurographics Association, pp. 147–153. 2

[OAIS09] OKABE M., ANJYO K., IGARASHI T., SEIDEL H.-P.: Animating pictures of fluid using video examples. *Computer Graphics Forum (Proc. EUROGRAPHICS 2009) 28*, 2 (2009), 677–686. 2

[OAO11] OKABE M., ANJYO K., ONAI R.: Creating fluid animation from a single image using video database. *Comput. Graph. Forum 30*, 7 (2011), 1973–1982. 2

[OCDD01] OH B. M., CHEN M., DORSEY J., DURAND F.: Image-based modeling and photo editing. In *Proceedings of the 28th annual conference on Computer graphics and interactive techniques* (New York, NY, USA, 2001), SIGGRAPH '01, ACM, pp. 433–442. 2, 5

[Ope13] OPENCV D. T.: OpenCV, cited September 2013. URL: http://opencv.org. 5, 7

[SMGG01] SLOAN P.-P. J., MARTIN W., GOOCH A., GOOCH B.: The lit sphere: a model for capturing npr shading from art. In *Graphics interface 2001* (2001), GI'01, pp. 143–150. 2

[SRLW13] SATYANAGA A., RAHARDJO H., LEONG E.-C., WANG J.-Y.: Water characteristic curve of soil with bimodal grain-size distribution. *Computers and Geotechnics 48*, 0 (2013), 51 – 61. 3

[TMPS03] TREUILLE A., MCNAMARA A., POPOVIĆ Z., STAM J.: Keyframe control of smoke simulations. *ACM Trans. Graph. 22*, 3 (July 2003), 716–723. 2

[WC07] WANG J., COHEN M. F.: Image and video matting: a survey. *Found. Trends. Comput. Graph. Vis. 3*, 2 (Jan. 2007), 97–175. 3

[WH97] WEI G.-Q., HIRZINGER G.: Parametric shape-from-shading by radial basis functions. *IEEE Trans. Pattern Anal. Mach. Intell. 19*, 4 (1997), 353–365. 6

[Wit05] WITELSKI T. P.: Motion of wetting fronts moving into partially pre-wet soil. *Advances in Water Resources 28*, 10 (2005), 1133 – 1141. 3

[WLZ*09] WANG H., LIAO M., ZHANG Q., YANG R., TURK G.: Physically guided liquid surface modeling from videos. *ACM Trans. Graph. 28*, 3 (July 2009), 90:1–90:11. 2

[WOBT09] WINNEMÖLLER H., ORZAN A., BOISSIEUX L., THOLLOT J.: Texture design and draping in 2d images. *Computer Graphics Forum 28*, 4 (July 2009), 1091–1099. 2

[WTL*06] WANG J., TONG X., LIN S., PAN M., WANG C., BAO H., GUO B., SHUM H.-Y.: Appearance manifolds for modeling time-variant appearance of materials. *ACM Trans. Graph. 25*, 3 (July 2006), 754–761. 2, 3

[XDR11] XUE S., DORSEY J., RUSHMEIER H.: Stone weathering in a photograph. In *Proceedings of the Twenty-second Eurographics conference on Rendering* (Aire-la-Ville, Switzerland, Switzerland, 2011), EGSR'11, Eurographics Association, pp. 1189–1196. 2

[XWT*08] XUE S., WANG J., TONG X., DAI Q., GUO B.: Image-based material weathering. *Computer Graphics Forum 27* (April 2008), 617–626. 2, 5

[YTBK11] YEUNG S. K., TANG C.-K., BROWN M. S., KANG S. B.: Matting and compositing of transparent and refractive objects. *ACM Transactions on Graphics 30*, 1 (2011), 2. 2

[ZTCS99] ZHANG R., TSAI P.-S., CRYER J., SHAH M.: Shape-from-shading: a survey. *Pattern Analysis and Machine Intelligence, IEEE Transactions on 21*, 8 (Aug 1999), 690–706. 5